Degradation Behavior of Polymeric Fire-Retardant Systems: A Case Study on TBOEP

Liu Fei[1,2], Lu Chenggang[2], Tang Yizhen[1,2,*] and Pan Yaru[3]

[1]*Innovation Institute for Sustainable Maritime Architecture Research and Technology, Qingdao University of Technology, 11 Fushun Road. Qingdao, Shandong, 266033 P.R. China*

[2]*School of Environmental and municipal engineering, Qingdao University of Technology, 777 Jialingjiang East Road. Qingdao, Shandong, 266520 P.R. China*

[3]*Tonghua Normal Collage, Yucai Roads 950, Tonghua, Jilin, 134000 P.R. China*

Abstract: With fireproofing function organophosphate flame retardants tri(2-butoxyethyl) phosphate (TBOEP) have been added into many polymeric materials widely. During applications of these polymeric fireproofing materials it was discharged into environment and causes serious problems to human and ecosystem. To reveal the degradation behaviour of TBOEP and its influence on environment, quantum chemical methods were employed to investigate the mechanisms, kinetics and toxicity of TBOEP in the atmosphere. Results indicate that OH radicals are more effective than ClO radicals to degrade TBOEP with H-abstraction mechanism dominating via low barriers less than 40 kJ/mol. Kinetically, as the temperature increases from 298 to 800 K, the total rate constant decreases gradually, and high temperature such as building-fire condition is unfavourable to degrade TBOEP. The degradation products exhibit significantly reduced acute and chronic toxicity to fish, daphnid and green algae. Moreover, mutagenicity toxicity is negative, while developmental toxicity increases in the degradation products. This work gives new insights into the environmental chemistry of polymeric fireproofing materials in the atmosphere.

Keywords: Fireproof polymeric material**,** Organophosphate flame retardant**,** Degradation**,** Kinetics**,** Ecotoxicity.

1. INTRODUCTION

As one kinds of fireproof material used widely in building, organophosphorus flame retardants (OPFRs) were used as additive into many building polymeric materials. However, during applications they present significant risks to both the ecological environment and human health. Driven by technological developments, OPFRs are used widely in plastic products, electronic appliances, textile materials, building materials, and so on [1-3]. As a kind of typical OPFRs, Tris(2-butoxyethyl) phosphate (TBOEP) is used commonly in floor decoration polymeric materials and industrial chemical product manufacturing [4]. It penetrates easily into environment and persists for long time [5, 6], and has been detected in various environmental media such as air and dust [7-19]. Moreover, TBOEP has neurotoxic, growth-inhibiting, and reproductive toxic effects on zebrafish [20-23]. Research indicates that TBOEP has carcinogenic potential, is present in human body fluids and biota, and forms metabolites in the human liver [24, 25]. As extensive applications and potential harm of polymeric materials in our daily life, TBOEP is necessary to be treated after released into environment. However, the attentions were not paid to this issue and possible influence of OPFRs in polymeric materials.

Generally, hydroxyl radicals (·OH) and chlorine monoxide radicals (·ClO) are considered to be the most important radicals promoting the degradation of organic pollutants[26]. Active hydroxyl radicals can oxidize and decompose persistent pollutants rapidly with the reaction rate constants being 10^8-10^{10} M^{-1} s^{-1} [27, 28]. The oxidative capacity was influenced by the reactants. For example, in reactions with dimethyl sulfoxide (DMSO)[29], the rate constant for ·OH is higher; while in the reactions with CH_3O_2 (methylperoxy radical), the rate constant for ·ClO is higher [30, 31]. Moreover, ·ClO exhibit low reaction energy barriers with various pollutants such as caffeine, ammonia nitrogen, and sesquiterpene compounds [32-35]. Noted that the concentration ·ClO is around 1.0×10^7 molecules·cm^{-3} in marine atmosphere [32]. Therefore, will the degradation by ·ClO on TBOEP be stronger than by ·OH in higher ·ClO concentration conditions?

Currently, researches on TBOEP focus on biodegradation [36] without the transformation mechanisms and ecological risks. During oxidative degradation in the atmosphere, the parent compound is oxidized into several intermediates, however, the toxicity of these intermediates is unclear. Given the widespread use of TBOEP in building fireproofing materials, temperature changes are a significant factor for its degradation. Existing data remain insufficient across a broader temperature range, particularly in extreme high-temperature conditions. To reveal these issues, combined approach of quantum chemical calculations and kinetic modelling was employed to

*Address Correspondence to this Author at the Innovation Institute for Sustainable Maritime Architecture Research and Technology, Qingdao University of Technology, 11 Fushun Road. Qingdao, Shandong, 266033 P.R. China; E-mail: tangyizhen@qut.edu.cn

Received on 11-11-2025 Accepted on 29-12-2025 Published on 07-01-2026

E-ISSN: 000-000/26

investigate the reaction mechanisms and kinetics of TBOEP degradation triggered by ·OH and ·ClO in atmosphere. Furthermore, through toxicity assessment, the ecological risks of TBOEP and its degradation products were comprehensively evaluated. It is expect to provide a theoretical basis to understand the variations of OPFRs in polymeric fire-retardant systems.

2. COMPUTATIONAL DETAILS

2.1. Reaction Mechanisms

All density functional theory (DFT) calculations were executed employing Gaussian 09 [37]. For geometric structure optimization, frequency analysis, and zero-point energy correctionon on reactants (R), products (P), intermediates (IM), and transition states (TS), the M06-2X/6-311++G(d,p) theoretical level was selected [38, 39]. It is known that the choice of theoretical method is important to the final result including geometrical parameters and energy. The reason to select M062X method lies on two aspects: firstly, M062X method shows better superiority in weak intramolecular interactions than the traditional density functional theory [40]; secondly, according to our many attempts, only the M062X method can describe all transition states in H-abstraction channels, while some of the transition states were not located using B3LYP method, which is common and popular in studying the reaction mechanisms. During the validation of computational result, all stationary points were confirmed. The minimum exhibits no imaginary frequencies, while the transition state has only one imaginary frequency. Additionally, to ensure that each transition state is correctly connected to the designed reactants and products, intrinsic reaction coordinate (IRC) calculations were performed at the same theoretical level [41]. Finally, to obtain more precise single-point energy for each stationary point, calculations were conducted at the M06-2X/6-311++G(3df,2pd) theoretical level based on the geometry from M06-2X/6-311++G(d,p) levels of theory.

2.2. Kinetics

To obtain more information about kinetics for degradation of TBOEP in the atmosphere, the rate constants were simulated using the Kinetic and Statistical Thermodynamics Package (KiSThelP) [42], along with correction for the empirical resonance frequency factor of 0.97. In addition, quantum tunneling effects were considered using the transition state theory (TST) and Wigner tunneling corrections (*X*). The formula for TST is as follows:

$$k^{\mathrm{TST}}(T) = \sigma \frac{k_B T}{h} \left(\frac{RT}{p^0}\right)^{\Delta n} e^{-\frac{\Delta G^{0,\ddagger}(T)}{k_B T}} \quad (1)$$

$$k = k^{\mathrm{TST}} \times X \quad (2)$$

k_B is the Boltzmann's constant; σ is the reaction path degeneracy; T is reaction temperature; RT/p^0 has the unit of the inverse of concentration; Δn is 1 for bimolecular reaction; h is the Planck's constant; and $\Delta G^{0,\ddagger}(T)$ represents the standard Gibbs free energy of activation for the reaction under consideration.

Moreover, the branching ratio of each pathway was calculated (Γ, defined as the ratio of the separated channel's rate constant to the total reaction rate constant) to assess its impact on the overall reaction. The formula is as follows:

$$\Gamma_i = \frac{k_i}{k_{tot}} \times \% \quad (3)$$

The degradation time was calculated using equation (4) in atmosphere, respectively, in which k is the overall rate constant; [*OH*] is the concentration of ·OH in the atmosphere.

$$\tau = \frac{1}{k \times [OH]} \quad (4)$$

2.3. Ecotoxicity Evaluation

The Ecological Structure Activity Relationships (ECOSAR) programme is a computerized version of the ECOSAR analysis programme adopted by the Office of Pollution Prevention and Toxic Substances (OPPT) [43]. The Toxicity Estimation Software Tool (T.E.S.T) is an online prediction system launched by the U.S. Environmental Protection Agency, which employs quantitative structure-activity relationship (QSAR) mathematical models [44]. T.E.S.T has multiple toxicity endpoints and can predict acute toxicity values based on the physical properties of molecular structures, making it used widely for toxicity prediction [44]. In this study, ECOSAR and T.E.S.T were employed to predict the potential acute toxic effects of TBOEP in aquatic ecosystems, involving aquatic organisms such as fish, daphnid, and green algae. For acute toxicity assessment, two key indicators were considered: 1) EC_{50} value for algae, which refers to the concentration that causes adverse effects in 50 % of green algae after 96 h of exposure; 2) LC_{50} value for fish and daphnid, where the LC_{50} value for fish or daphnid refers to the concentration that causes 50 % mortality in fish or daphnid after 96 h of exposure. To assess the long-term toxic potential of TBOEP and its degradation products comprehensively and thoroughly, the chronic toxicity (ChV) values were calculated. Additionally, considering the potential multifaceted health impacts of these substances,

predictive analysis of the developmental toxicity and mutagenicity of TBOEP and its degradation products was conducted.

3. RESULTS AND DISCUSSIONS

3.1. Preliminary Reactions of ·OH with TBOEP in the Atmosphere

The molecular structures of ·OH, ·ClO, and TBOEP were shown in Figure **1**. The structural feature of TBOEP lies in its central phosphate group, which is connected to three n-butyl groups via ester bonds, forming a highly symmetrical tridentate structure. This structural symmetry endows TBOEP with remarkable environmental stability, enabling it to resist degradation processes such as photolysis or hydrolysis. The electrostatic potential surfaces (ESP) of ·ClO, ·OH, and TBOEP were calculated and shown in Figure **1**. It can be seen that the O atom from the P=O bond shows a more prominent red color. In ESP, red indicates a negative charge, and a darker shade means a larger absolute value of the atom. Since multiple O atoms are connected to the P atom, electrons are mostly confined in P-O bonds, making addition reactions difficult to occur. ·OH and ·ClO are electronegative, implying that substitution reactions can easily take place in the regions connected to O. The weak C-H bonds in the alkyl chains (especially the α-H adjacent to heteroatoms) are the main sites for H-abstraction reactions by ·OH. Moreover, the average local ionization energy (ALIE) of the TBOEP molecule was analyzed using the Multiwfn (V3.7) software [45, 46] to predict its main reaction sites, and it was shown in Figure **1**, as well. In the surface the smaller the ALIE value, the weaker the electron bonding force or the stronger the electron activity, making it more prone to electrophilic reactions and radical reactions. The ALIE values in the blue regions are lower than those in the red regions, indicating stronger electron activity and higher reactivity with electrophilic reagents. The darker the colour, the higher the reaction probability. Study on tris(2-chloroethyl) phosphate (TCEP) degradation presumed two pathways via addition of ·OH to the P atom and the attack of ·OH at the branched chain terminal C atoms to generate carbon-centred radicals [47]. Since TCEP and TBOEP have similar structures, it is assumed that they undergo similar reactions.

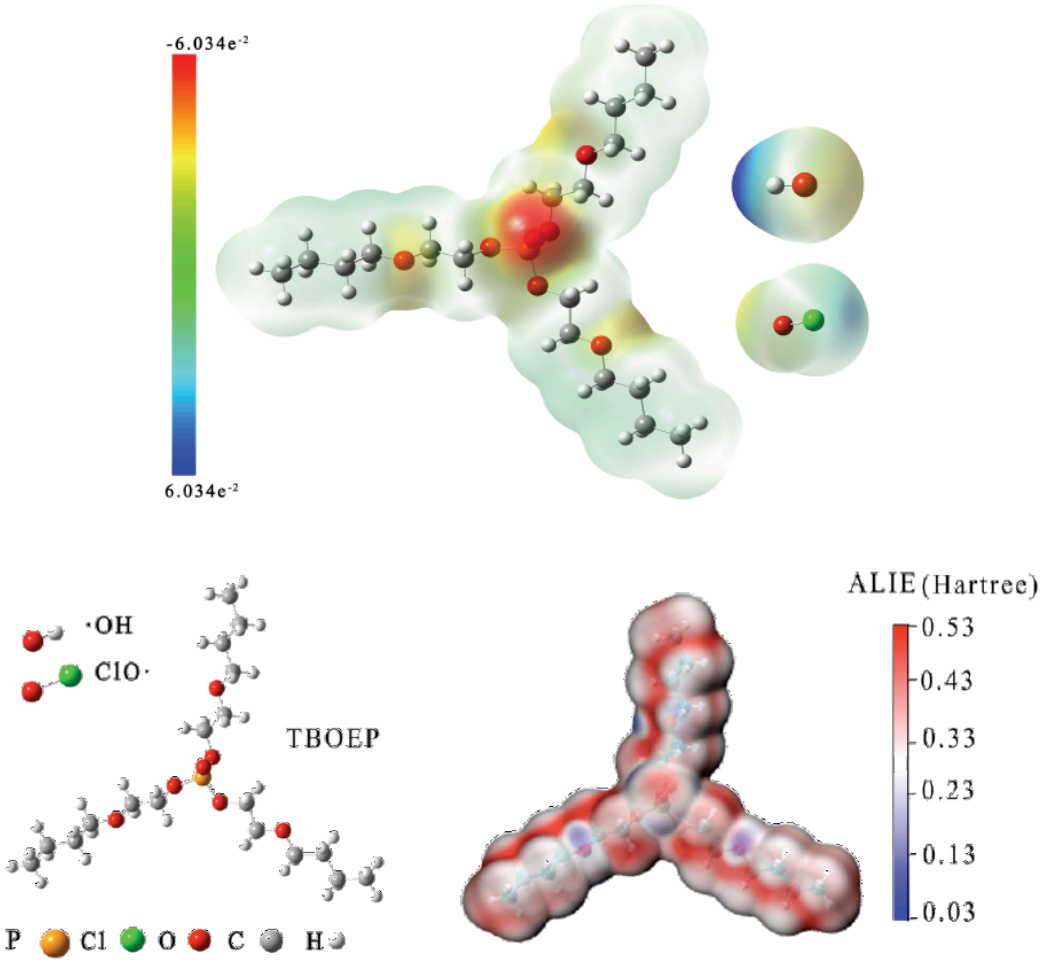

Figure 1: The structures and electrostatic potential surfaces (ESP) of tri(2-butoxyethyl) phosphate (TBOEP), ·OH and ·ClO and average localized ionization energy (ALIE) values for TBOEP.

The progress of the reaction was shown in Figure **2** to give a clear description. To gain deeper understanding on the degradation behaviour of TBOEP under free radical attack, supporting information provide detailed data on reaction energy barriers, thermodynamic parameters, and optimized geometric structures of intermediates and transition states. The optimized geometries for all species were shown in Figure **S1**(Supporting information). Detailed energy was listed in Tables **S1**.

3.1.1. Hydrogen-Abstraction Mechanism

TBOEP contains multiple C-H bonds, and these hydrogen atoms can be attacked and extracted easily by free radicals. According to structure of TBOEP, there are six types of H atom exist as shown in Figure **2**, *i.e.*, one methyl-H and five different methylene-H. Therefore, H-abstraction reactions can occur via the following channels:

TBOEP + ·OH → TA-TS-1 → TA-P1 + H_2O (R1)

TBOEP + ·OH → TA-TS-2 → TA-P2+ H_2O (R2)

TBOEP + ·OH → TA-TS-3 → TA-P3 + H_2O (R3)

TBOEP + ·OH → TA-TS-4 → TA-P4+ H_2O (R4)

TBOEP + ·OH → TA-TS-5 → TA-P5+ H_2O (R5)

TBOEP + ·OH → TA-TS-6 → TA-P6 + H_2O (R6)

Based on the structure of branched chain ($-OCH_2CH_2OCH_2CH_2CH_2CH_3$) in TBOEP, the activity of these H atoms shows significant differences. Energetically, the energy barrier required in R1 channel is 36.8 kJ/mol. The energy barriers required to extract adjacent methylene hydrogens are 14.1 (TA-TS-2) and 25.5 (TA-TS-3) kJ/mol, respectively, with R2 channel being the lowest energy pathway among all channels. Therefore, the most active site is the methylene hydrogen adjacent to ether oxygen as shown in Figure **2**. This may be due to the electron-withdrawing effect of the ether oxygen. While in channels of R4 and R5, the β-H and γ-H ($-CH_2-CH_2-CH_3$) at the terminal butoxy group are extracted with the energy barrier being 29.0 and 28.9 kJ/mol. Noted H atoms abstracted in R4 and R5 channels locating in the end of the molecular chain, are distant from polar groups and affected slightly by steric hindrance to have slightly lower bond energies, making them more susceptible to be attacked by radicals. Finally, H atom from the terminal methyl group extracted via R6 channel undergoes with an energy barrier of 38.8 kJ/mol, the highest one among all channels. It is speculated that the higher energy barrier comes from higher bond energy and the absence of

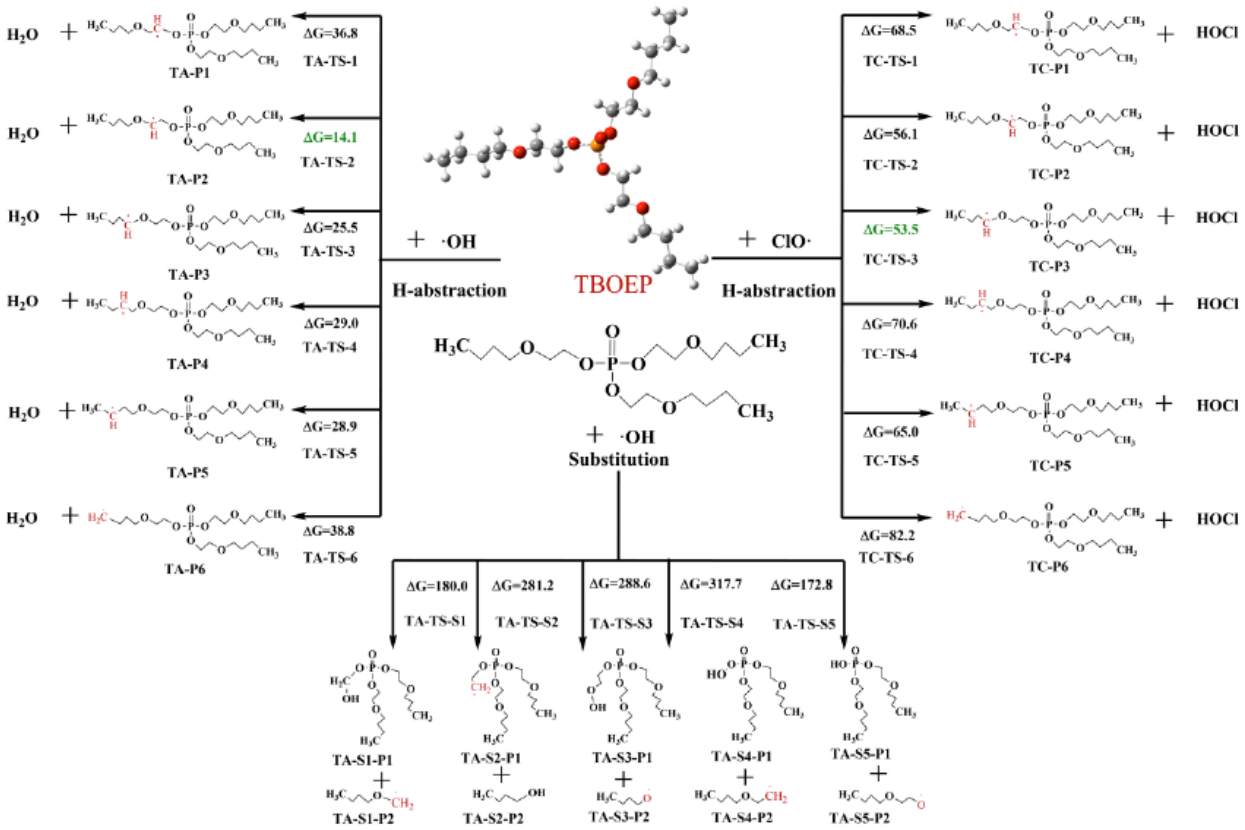

Figure 2: Diagram of the channels in the reactions of TBOEP with ·OH and ·ClO at M06-2X/6-311++G (3df,2pd) // M06-2X/6-311+G(d,p) level. For ΔG (unit in kJ/mol).

activating groups, which results in lower reaction activity.

To sum up, in the reaction between ·OH and TBOEP, all H-abstraction pathways surpassing barriers lower than 40 kJ/mol, and they are possible to take place in the atmosphere. With the lowest energy barriers, the most feasible pathway is R2 with the hydrogen from middle methylene next to O atom in ether, which are electron-donating group.

3.1.2. Substitution Mechanism

Besides H-abstraction mechanisms, substitution reactions represent a typical degradation route for TBOEP. Based on result that five substitution pathways were systematically identified through the following ways:

TBOEP + ·OH → TA-TS-S1 → TA-S1-P1+TB-S1-P2 (R7)

TBOEP + ·OH → TA-TS-S2 → TA-S2-P1+TA-S2-P2 (R8)

TBOEP + ·OH → TA-TS-S3 → TA-S3-P1+TA-S3-P2 (R9)

TBOEP + ·OH → TA-TS-S4→ TA-S4-P1+TA-S4-P2 (R10)

TBOEP + ·OH → TA-TS-S5 → TA-S5-P1+TA-S5-P2 (R11)

Based on the special structure of TBOEP, it is speculated that the substitution reactions mainly focus on the C-O and P-O bond. The P-O bond has the lowest bond energy, while the C-O bond has the strongest polarity, making it as the preferred target for the substitution by ·OH. As seen in Figure **2**, ·OH attack the C atom in C-O bond connecting with P atom, the O atom in C-O bond at the butoxy end to form butyl or butyl hydroperoxide, the O and P atom in P-O bond lead to several products, respectively, in channels of R7 to R11. The corresponding energy barriers surmounting are 180.0, 281.2, 288.6, 317.7 and 172.8 kJ/mol, obviously, with high barriers all the channels are difficult to undergo in the atmosphere, implying that the substitution processes of TBOEP are restricted.

Moreover, it was proposed that phosphorus and oxygen atoms within the phosphorus-oxygen double bond (P=O) may function as reactive sites for hydroxyl radicals. Thus, M06-2X/6-311++G(d,p) calculation was performed to visualize the average local ionization energy (ALIE) distribution in TBOEP (Figure **1**). The result indicates that the region surrounding the phosphorus atom is predominantly characterized by red-white coloration (high ALIE values). And it is conceivable that addition mechanism was unfavorable.

To sum up, with lower energy barriers H-abstraction channels serve as the primary reaction pathway. While substitution reactions necessitate surmounting relatively high energy barriers, making them difficult to proceed spontaneously under conventional conditions.

3.2. Reaction of · ClO with TBOEP in the Atmosphere

Based on analysis of the reaction between ·OH with TBOEP, it can be concluded that H-abstraction mechanism is dominant. Considering the similarity between the reactions of ·OH and ·ClO with organics, only H-abstraction mechanism in the reactions of TBOEP and ·ClO was studied, and the reaction progress was shown in Figure **2**, as well, to give a clear and comparable description. The optimized geometries for all species were shown in Figure **S2**. Detailed energy was listed in Tables **S2**. As for the reaction of TBOEP with ·ClO, six H-abstraction pathways take place as follows:

TBOEP + ClO· → TC-TS-1 → TC-P1 + HOCl (R12)

TBOEP + ClO· → TC-TS-2 → TC-P2 + HOCl (R13)

TBOEP + ClO· → TC-TS-3 → TC-P3 + HOCl (R14)

TBOEP + ClO· → TC-TS-4 → TC-P4 + HOCl (R15)

TBOEP + ClO· → TC-TS-5 → TC-P5 + HOCl (R16)

TBOEP + ClO· → TC-TS-6 → TC-P6 + HOCl (R17)

The energy barriers for the six pathways R12 to R17 are 68.5, 56.1, 53.5, 70.6, 65.0, and 82.2 kJ/mol, respectively, suggesting that the reactivity of ·ClO to abstract hydrogen from TBOEP exhibits significant dependency. It is mentioned that the barriers are significantly higher than those in the reaction between ·OH and TBOEP, indicating that·OH have greater oxidative capacity toward TBOEP than ·ClO. It is assumed that chlorine in ·ClO has lower electronegativity than the oxygen in ·OH. Noted that lower energy barriers correspond to the two hydrogen atoms adjacent to the acyl oxygen, in accordance with that in the reaction of ·OH. Since ·OH are the primary atmospheric scavengers of air pollutants [48], it is anticipated that the feasibility of ·OH to degrade

TBOEP under atmospheric conditions is higher than that of ·ClO.

3.3. Subsequent Reactions of H-Abstraction Mechanism Products in Atmosphere

Based on above result it can be concluded clearly that H-abstraction channels compass lower energy barriers, demonstrating highly feasible chemical conversion pathways to generate highly reactive products TA-P1 to TA-P6. The remaining unpaired electrons in these products confer them with strong oxygen affinity and nitrogen oxide capture capabilities. In atmospheric environment, these highly activated products can undergo subsequent reactions with key atmospheric components. Thus further reactions of these products with O_2 and NO were investigated. The subsequent processes were shown in Figure **3**, the relative energy was listed in Table **S3**, and the optimized geometries were shown in Figure **S3**.

Firstly, these products react with O_2 via barrierless addition steps to form peroxyl radicals (ROO·) rapidly at typical atmospheric condition. As seen TA-P1 to TA-P6 react with O_2 in the atmosphere, respectively, to form TAP1-IM-1to TAP6-IM-1. Their stabilization energies are 256.2, 253.0, 264.4, 253.4, 257.8, and 258.4 kJ/mol, respectively. These intermediates then undergo addition reactions with NO leading to TAP1-IM-2, TAP2-IM-2, TAP3-IM-2, TAP4-IM-2, TAP5-IM-2, and TAP6-IM-2, respectively, via barrier-free processes. TAP1-IM-2 eliminates NO_2 to form TAP1-1, which is exothermic and occurs easily in typical atmosphere. Subsequently, TAP1-1 undergoes decomposition via TA-TS1(1) to form TAP1-2 and TAP1-3, with a energy barrier of 76.7 kJ/mol. The reaction process from TAP2-IM-2 is similar to that of the aforementioned TAP1-IM-2, eliminating NO_2 to form TAP2-1, and then undergoes decomposition via TA-TS2(1) to form TAP2-2 and TAP2-3 requiring a energy barrier of 12.8 kJ/mol. For TAP3-IM-2, TAP4-IM-2, TAP5-IM-2, and TAP6-IM-2, they also undergo exothermic steps to eliminate NO_2, producing TAP3-1, TAP4-1, TAP5-1, and TAP6-1, respectively. TAP3-1 dissociates to form TAP3-2 and TAP3-3 via TA-TS3(1) with a energy barrier of 6.5 kJ/mol, which is easily to be surpassed. TAP4-1, TAP5-1 and TAP6-1 take place similar decomposition to from TAP4-2 + TAP4-3, TAP5-2 + TAP5-3 and TAP6-2 + TAP6-3, respectively, with energy barriers being 24.7, 53.9 and 63.5 kJ/mol.

In term of energy barrier, the final products including TAP2-2 + TAP2-3, TAP3-2 + TAP3-3 and TAP4-2 + TAP4-3 are easily to be formed in the subsequent processes, accompanying the formation of typical atmospheric pollutants such as NO_2.

3.4. Kinetics of ·OH with TBOEP

To better understand the degradation and transformation processes of TBOEP in environment, KiSThelP program was used to calculate precisely the rate constants at different temperatures in the

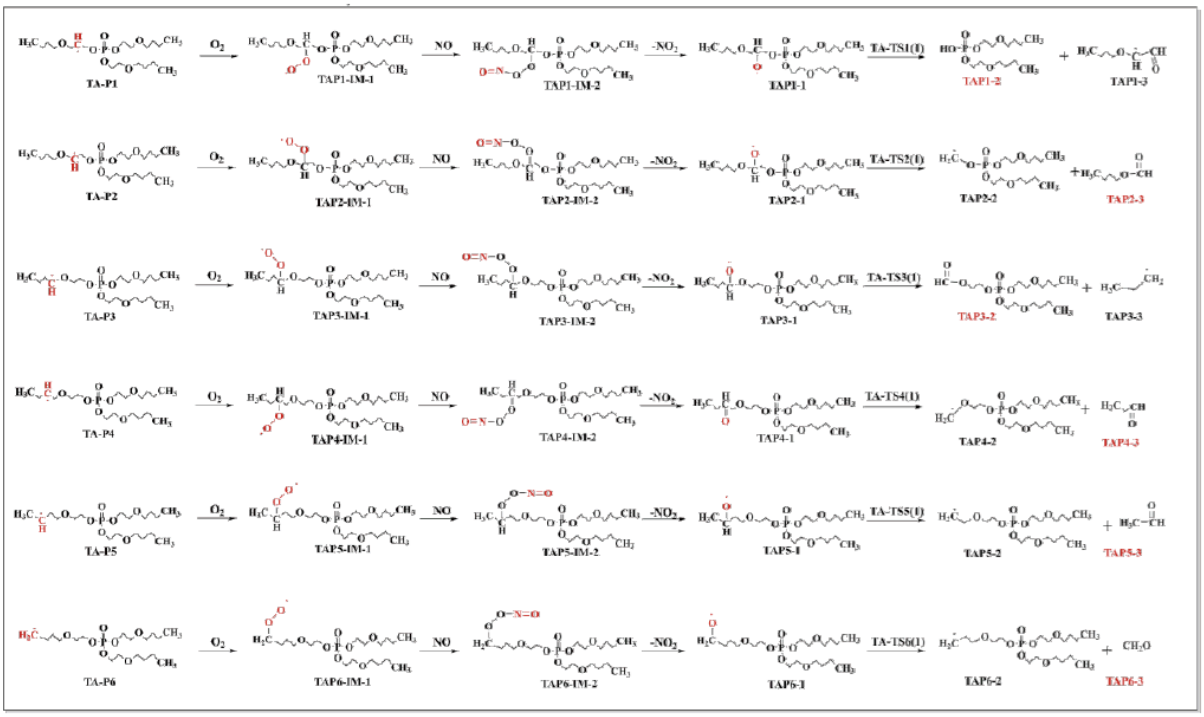

Figure 3: Subsequent reactions of main degradation products from ·OH-initiated degradation of TBOEP with O_2 and NO in the atmosphere.

atmosphere. The branching ratio and lifetime (half-life) was also evaluated. Because the the reaction energy barrier for ·ClO is relatively high, and it was assumed that the rate constant is relatively slow, thus the kinetics in the reaction of TBOEP with ·ClO was out of consideration here. For the reaction between TBOEP and ·OH, substitution channels are difficult to occur with high barriers, and therefore only the contribution of H-abstraction pathways to the overall reaction was considered. The result were shown in Figure **4**. Table **1** lists the detailed rate constants and branching ratios for each channel at 298 K.

Considering the temperature of the flame in a fire, the total rate constant (k_{tot}) and branched rate constants ($k_{H\text{-}n}$) were calculated for the temperature range from 298 K to 800 K in the atmosphere. As shown in Figure **4**, in typical atmospheric conditions (T = 298 K and 1 atm), the rate constants for six H-abstraction channels are 6.15×10^{-13}, 2.29×10^{-9}, 2.11×10^{-11}, 6.89×10^{-12}, 3.97×10^{-12}, and 6.49×10^{-14} cm^3 $molecule^{-1}$ s^{-1}, respectively. The rate constant of R2 ($k_{H\text{-}2}$) accounts for 98.93 % to the overall reaction, while the contributions of other pathways are negligible. Additionally, it was noted that temperature influences the total rate constant obviously. As the temperature increases from 298 to 800 K, the total rate constant decreases gradually from 2.95×10^{-9} to 5.55×10^{-11} cm^3 $molecule^{-1}$ s^{-1}. The rate constants caused by temperature differences happens due to fires or variations in altitude, And the residence time and spatial distribution characteristics of pollutants in the atmosphere will be influenced significantly. At 298 K and ·OH concentration of 1.0×10^6 molecules·cm^{-3}, the estimated atmospheric lifetime of TBOEP is 0.09 h, indicating that ·OH can degrade TBOEP rapidly in the atmosphere. As temperature increases from 298 to 800 K, the atmospheric lifetime also increases gradually. At higher temperatures (508 K), the half-life extends to approximately 5.52 h, meaning that TBOEP degrades

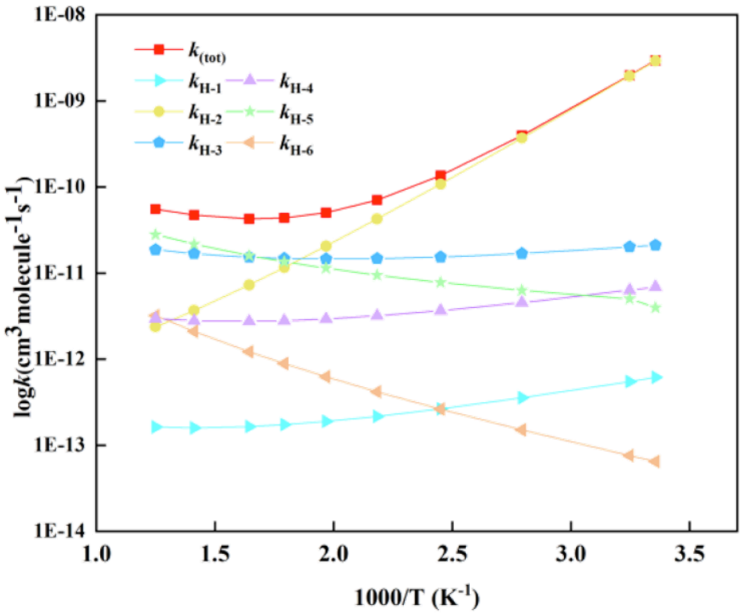

Figure 4: The calculated rate constants in the reaction of TBOEP with ·OH along with temperature (T) at 1 atm.

Table 1: The Total and Separated Rate Constant k (cm^3 $molecule^{-1}s^{-1}$) and Branch Ratio (*Γ*) in the Reaction of TBOEP with ·OH at 298 K in the Atmosphere

Channels	*k*	*Γ*(%)
TBOEP + ·OH→TA-TS-1($k_{H\text{-}1}$)	6.15×10^{-13}	0.02
TBOEP + ·OH→TA-TS-2($k_{H\text{-}2}$)	2.92×10^{-9}	98.93
TBOEP + ·OH→TA-TS-3($k_{H\text{-}3}$)	2.11×10^{-11}	0.72
TBOEP + ·OH→TA-TS-4($k_{H\text{-}4}$)	6.89×10^{-12}	0.23
TBOEP + ·OH→TA-TS-5($k_{H\text{-}5}$)	2.97×10^{-12}	0.10
TBOEP + ·OH→TA-TS-6($k_{H\text{-}6}$)	6.49×10^{-14}	0.00
TBOEP + ·OH(k_{tot})	2.95×10^{-9}	100

more slowly at higher temperatures and requires longer time to be removed. Previous study on the degradation of tris(2-chloroisopropyl) phosphate initiated by ·OH showed that the rate constant is 1.7 $\times 10^{-10}$ cm^3 $molecule^{-1}$ s^{-1} at 298 K in the atmosphere [49], which is close to that in this work, indicating that ·OH might degrade organophosphate flame retardants quickly. Therefore, it can be assumed that in high temperature such as fire conditions, the degradation rate becomes slower and then the polymeric materials will be protected with TBOEP as additive. However, the physical characteristic and mechanical strength might be changed.

3.5. Ecotoxicity Assessment

During degradation of TBOEP various intermediates and products can be formed. Employing ECOSAR and T.E.S.T models were used to assess the developmental toxicity, mutagenicity, acute and chronic toxicity of the parent compound, primary intermediates and transformation products when exposed to three representative aquatic organisms (*i.e.*, fish, daphnid, and green algae). Figure **5a** and **5b** show the acute and chronic toxicity assessments of TBOEP, TAP1-IM-2, TAP2-IM-2, TAP3-IM-2, TAP4-IM-2, TAP5-IM-2, TAP6-IM-2, TAP1-2, TAP2-3, TAP3-2, TAP4-3, TAP5-3, and TAP6-3. Figure **5c** shows the assessment of developmental toxicity and mutagenicity for these selected compounds. Table **S4** provides detailed acute and chronic toxicity values.

As shown in figures, the predicted acute toxicity of TBOEP to fish, daphnid, and green algae ($logLC_{50}$ or $logEC_{50}$) are 1.62, 1.42, and 1.45 mg/L, respectively, and all are below 2 mg/L,indicating that TBOEP is acute toxicity. The predicted chronic toxicity of TBOEP for fish, daphnid, and green algae (logChV) are 0.66, 0.52, and 0.96 mg/L, respectively, which are below 1 mg/L, indicating that it is chronic toxicity. Therefore, TBOEP exhibits both acute and chronic toxicity to these three aquatic organisms. On the other hand, from the evaluated values it can be seen that the acute and chronic toxicity of TAP1-IM-2, TAP2-IM-2, TAP3-IM-2, TAP4-IM-2, TAP5-IM-2, and TAP6-IM-2 were reduced slightly. The acute toxicity values of TAP1-2, TAP2-3, TAP3-2, TAP4-3, TAP5-3, and TAP6-3 are greater than 2 mg/L, and the chronic toxicity values are greater

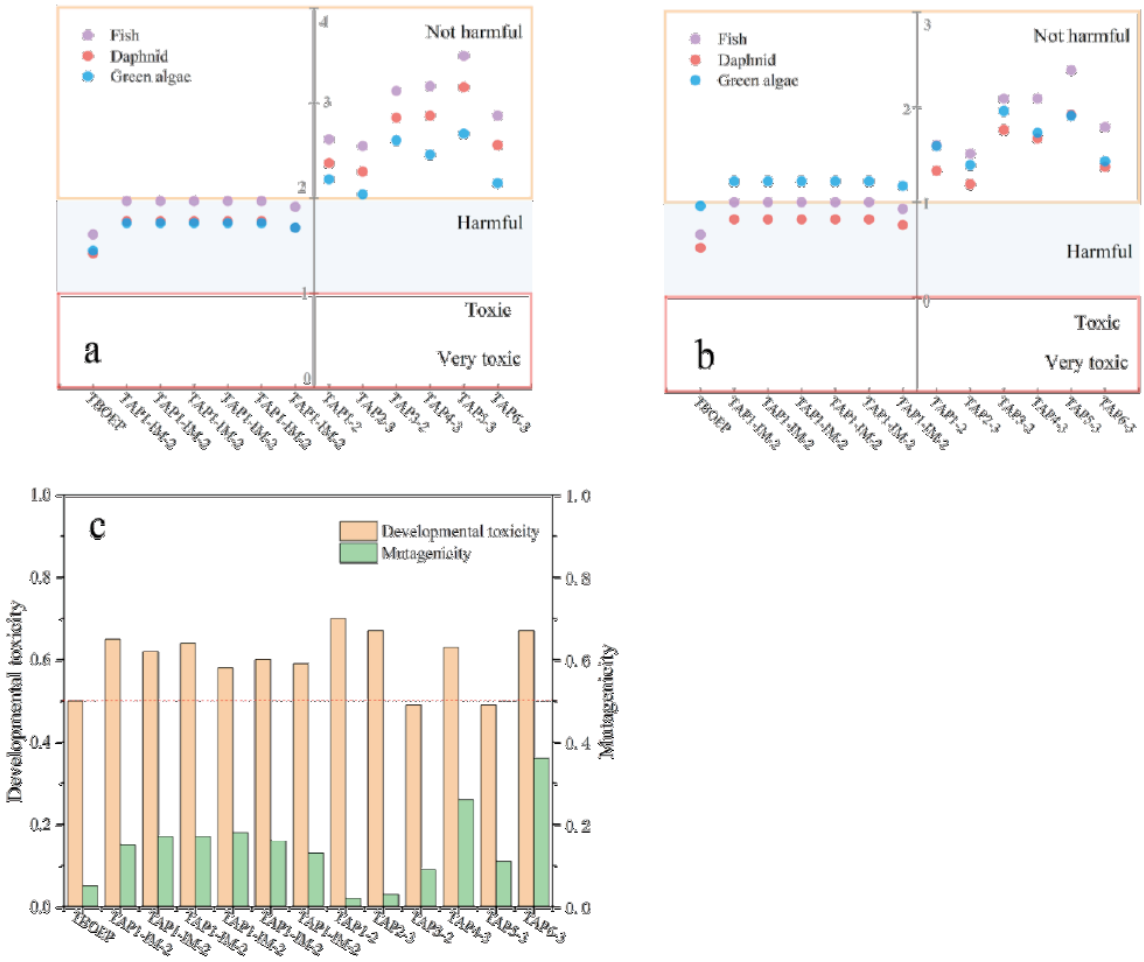

Figure 5: Developmental toxicity, mutagenicity, and ecological toxicity values ($logLC_{50}$, $logEC_{50}$, and logChV) of TBOEP and its degradation products for fish, daphnid, and green algae (uniting mg/L). (**a**) is acute toxicity, (**b**) is chronic toxicity, and (**c**) is developmental toxicity and mutagenicity.

than 1 mg/L, reaching the non-toxic standard. And thus these products are harmless to the three aquatic organisms. Generally, compounds are classified into developmental toxicants (developmental toxicity > 0.5 mg/L) and developmental non-toxicants (developmental toxicity < 0.5 mg/L); mutagenicity negative (ames mutagenicity < 0.5) and mutagenicity positive (ames mutagenicity > 0.5). As shown in Figure **5c**, except for TAP3-2 and TAP5-3, the developmental toxicity values of all compounds are greater than 0.5 mg/L, indicating that they all exhibit developmental toxicity. For the parent compound, all intermediates and degradation products, the mutagenicity values are less than 0.5 mg/L, indicating that they do not exhibit mutagenicity. In summary, TBOEP exhibits acute and chronic toxicity to fish, daphnid, and green algae. The degradation and transformation products meet non-toxic standards and it is assumed that they are harmless to the three aquatic organisms. Most of the compounds exhibit developmental toxicity; the parent compound, all intermediates and degradation products are non-mutagenic. The toxicity implies that the degradation by ·OH is beneficial to the environment after it was emitted or discharged into environment, and it can propose theoretical information for the recycle and waste management of these polymeric materials.

4. CONCLUSIONS

To understand the chemical behavior of additive fireproof compounds in polymeric materials, the mechanism, kinetics, and toxicity of the degradation of TBOEP by ·OH and ·ClO in environment were investigated theoretically. Results indicate that ·OH is more effective than ·ClO to degrade TBOEP, with the H-abstraction mechanism being dominant. In ·OH with TBOEP reaction the six H-abstraction pathways overcome energy barriers of 36.8, 14.1, 25.5, 29.0, 28.9 and 38.8 kJ/mol in the atmosphere. While substitution channels are difficult to occur. Moreover, kinetic data indicates that high temperatures is unfavourable to degrade TBOEP, and thus it is assumed that the polymeric materials can be protected in fire conditions. The acute and chronic toxicity of degradation products to all three aquatic organisms is reduced, and mutagenicity is negative, while developmental toxicity of the degradation products is positive. The toxicity implies that the degradation by ·OH is beneficial to the environment after it was emitted or discharged into environment.

CREDIT AUTHORSHIP CONTRIBUTION STATEMENT

Fei Liu: Investigation, Writing – original draft, Formal analysis. **Chenggang Lu**: Formal analysis, Data curation, Writing – review & editing. **Yizhen Tang**: Writing – review & editing. Supervision, Conceptualization, Funding acquisition. **Yaru Pan**: Writing – review & editing, Funding acquisition.

DECLARATION OF COMPETING INTEREST

The authors declare that they have no known competing financial interests or personal relationships that could have appeared to influence the work reported in this paper.

ACKNOWLEDGEMENT

This work has been supported by the Natural Science Foundation of Shandong Province (ZR2024MB073) and the Natural Science Foundation of Jilin Province (20220101076JC).

REFERENCES

[1] Li S, Zhu F, Zhang D, *et al*. Seasonal concentration variation and potential influencing factors of organophosphorus flame retardants in a wastewater treatment plant. Environ Res. 2021; 199: 111318. https://doi.org/10.1016/j.envres.2021.111318

[2] Yao C, Yang H, Li Y. A review on organophosphate flame retardants in the environment: Occurrence, accumulation, metabolism and toxicity. Sci Total Environ. 2021; 795: 148837. https://doi.org/10.1016/j.scitotenv.2021.148837

[3] Li J, Zhao L, Letcher RJ, *et al*. A review on organophosphate Ester (OPE) flame retardants and plasticizers in foodstuffs: Levels, distribution, human dietary exposure, and future directions. Environ Int. 2019; 127: 35-51. https://doi.org/10.1016/j.envint.2019.03.009

[4] Liang Y, Zhou X, Wu Y, *et al*. Meta-omics elucidates key degraders in a bacterial tris(2-butoxyethyl) phosphate (TBOEP)-degrading enrichment culture. Water Res. 2023; 233: 119774. https://doi.org/10.1016/j.watres.2023.119774

[5] Rodríguez I, Calvo F, Quintana JB, *et al*. Suitability of solid-phase microextraction for the determination of organophosphate flame retardants and plasticizers in water samples. J Chromatogr A. 2006; 1108: 158-165. https://doi.org/10.1016/j.chroma.2006.01.008

[6] Wang Y, Kannan P, Halden RU, *et al*. A nationwide survey of 31 organophosphate esters in sewage sludge from the United States. Sci Total Environ. 2019; 655: 446-453. https://doi.org/10.1016/j.scitotenv.2018.11.224

[7] Xu L, Hu Q, Liu J, *et al*. Occurrence of organophosphate esters and their diesters degradation products in industrial wastewater treatment plants in China: Implication for the usage and potential degradation during production processing. Environ Pollut. 2019; 250: 559-566. https://doi.org/10.1016/j.envpol.2019.04.058

[8] Harrad S, Brommer S, Mueller JF. Concentrations of organophosphate flame retardants in dust from cars, homes, and offices: An international comparison. Emerg Contam. 2016; 2: 66-72. https://doi.org/10.1016/j.emcon.2016.05.002

[9] Han X, Hao Y, Li Y, *et al*. Occurrence and distribution of organophosphate esters in the air and soils of Ny-Ålesund and London Island, Svalbard, Arctic. Environ Pollut. 2020; 263: 114495. https://doi.org/10.1016/j.envpol.2020.114495

[10] He H, Gao Z, Zhu D, *et al*. Assessing bioaccessibility and bioavailability of chlorinated organophosphorus flame retardants in sediments, Chemosphere. 2017; 189: 239-246. https://doi.org/10.1016/j.chemosphere.2017.09.017

[11] Quintana JB, Rodil R, Reemtsma T. Determination of phosphoric acid mono-and diesters in municipal wastewater by solid-phase extraction and ion-pair liquid chromatography-tandem mass spectrometry. Anal Chem. 2006; 78: 1644-1650. https://doi.org/10.1021/ac0517186

[12] Khairy MA, Lohmann R, Organophosphate flame retardants in the indoor and outdoor dust and gas-phase of Alexandria. Egypt. Chemosphere. 2019; 220: 275-285. https://doi.org/10.1016/j.chemosphere.2018.12.140

[13] Bollmann UE, Möller A, Xie Z, *et al*. Occurrence and fate of organophosphorus flame retardants and plasticizers in coastal and marine surface waters. Water Res. 2012; 46: 531-538. https://doi.org/10.1016/j.watres.2011.11.028

[14] Kim UJ, Kannan K, Occurrence and distribution of organophosphate flame retardants/plasticizers in surface waters,tap water, and rainwater: Implications for human exposure. Environ Sci Technol. 2018; 52: 5625-5633. https://doi.org/10.1021/acs.est.8b00727

[15] Lee S, Cho HJ, Choi W, *et al*. Organophosphate flame retardants (OPFRs) in water and sediment: Occurrence, distribution, and hotspots of contamination of Lake Shihwa, Korea. Mar Pollut Bull. 2018; 130：105-112. https://doi.org/10.1016/j.marpolbul.2018.03.009

[16] Lee S, Jeong W, Kannan K, *et al*, Occurrence and exposure assessment of organophosphate flame retardants (OPFRs) through the consumption of drinking water in Korea. Water Res. 2016; 103: 182-188. https://doi.org/10.1016/j.watres.2016.07.034

[17] Luo Z, Huang W, Yu W, *et al*. Insights into electrochemical oxidation of tris(2-butoxyethyl) phosphate (TBOEP) in aquatic media: Degradation performance, mechanisms and toxicity changes of intermediate products. Chemosphere. 2023; 343: 140267. https://doi.org/10.1016/j.chemosphere.2023.140267

[18] Wan W, Zhang S, Huang H, *et al*. Occurrence and distribution of organophosphorus esters in soils and wheat plants in a plastic waste treatment area in China. Environ Pollut. 2016; 214: 349-353. https://doi.org/10.1016/j.envpol.2016.04.038

[19] Wang Y, Li Z, Tan F, *et al*. Occurrence and air-soil exchange of organophosphate flame retardants in the air and soil of Dalian, China. Environ Pollut. 2020; 265: 114850. https://doi.org/10.1016/j.envpol.2020.114850

[20] Xu Q, Wu D, Dang Y, *et al*. Reproduction impairment and endocrine disruption in adult zebrafish (Danio rerio) after waterborne exposure to TBOEP. Aquat Toxicol. 2017; 182: 163-171. https://doi.org/10.1016/j.aquatox.2016.11.019

[21] Jiang F, Liu J, Zeng X, *et al*, Tris (2-butoxyethyl) phosphate affects motor behavior and axonal growth in zebrafish (Danio rerio) larvae. Aquat Toxicol. 2018; 198: 215-223. https://doi.org/10.1016/j.aquatox.2018.03.012

[22] Egloff C, Crump D, Porter E, *et al*. Tris(2-butoxyethyl)phosphate and triethyl phosphate alter embryonic development, hepatic mRNA expression, thyroid hormone levels, and circulating bile acid concentrations in chicken embryos. Toxicol Appl Pharmacol. 2014; 279: 303-310. https://doi.org/10.1016/j.taap.2014.06.024

[23] Eng ML, Letcher RJ, Williams TD, *et al*. In ovo tris(2-butoxyethyl) phosphate concentrations significantly decrease in late incubation after a single exposure via injection, with no evidence of effects on hatching success or latent effects on growth or reproduction in zebra finches. Environ Toxicol Chem. 2017; 36: 83-88. https://doi.org/10.1002/etc.3502

[24] Van den Eede N, De Meester I, Maho W, *et al*. Biotransformation of three phosphate flame retardants and plasticizers in primary human hepatocytes: untargeted metabolite screening and quantitative assessment. J Appl Toxicol 2016; 36: 1401-1408. https://doi.org/10.1002/jat.3293

[25] Yu D, Hales BF, Robaire B. Organophosphate ester flame retardants and plasticizers affect the phenotype and function of HepG2 liver cells. Toxicol Sci. 2024; 199: 261-275. https://doi.org/10.1093/toxsci/kfae034

[26] Liou SY, Dodd MC. Evaluation of hydroxyl radical and reactive chlorine species generation from the superoxide/hypochlorous acid reaction as the basis for a novel advanced oxidation process. Water Res. 2021; 200: 117142. https://doi.org/10.1016/j.watres.2021.117142

[27] Han SK, Nam SN, Kang JW. OH radical monitoring technologies for AOP advanced oxidation process. Water Sci Technol. 2002; 46: 7-12. https://doi.org/10.2166/wst.2002.0709

[28] Oturan MA, Aaron JJ. Advanced oxidation processes in water/wastewater treatment: Principles and applications. A Review. Crit Rev Environ Sci Technol. 2014; 44: 2577-2641. https://doi.org/10.1080/10643389.2013.829765

[29] Martínez E, Aranda A, Díaz de Mera Y, *et al*. Atmospheric DMSO degradation in the gas phase: Cl−DMSO reaction. Temperature dependence and products. Environ Sci Technol. 2002; 36: 1226-1230. https://doi.org/10.1021/es010169s

[30] Assaf E, Sheps L, Whalley L, *et al*. The reaction between CH_3O_2 and OH radicals: Product yields and atmospheric implications. Environ Sci Technol. 2017; 51: 2170-2177. https://doi.org/10.1021/acs.est.6b06265

[31] Ward MK, Rowley DM. Kinetics of the ClO+ CH_3O_2 reaction over the temperature range T= 250-298 K. Phys Chem Chem Phys. 2016; 18: 13646-13656. https://doi.org/10.1039/C6CP00724D

[32] Chang CT, Liu TH, Jeng FT. Atmospheric concentrations of the Cl atom, ClO radical, and HO radical in the coastal marine boundary layer. Environ Res. 2004; 94: 67-74. https://doi.org/10.1016/j.envres.2003.07.008

[33] Guo K, Wu Z, Yan S, *et al*. Comparison of the UV/chlorine and UV/H_2O_2 processes in the degradation of PPCPs in simulated drinking water and wastewater: Kinetics, radical mechanism and energy requirements. Water Res. 2018; 147: 184-194. https://doi.org/10.1016/j.watres.2018.08.048

[34] Wu H, Zhang S, Dang J, *et al*. A first comprehensive insight into the sesquiterpene oxidation and sequential HOMs formation in the marine atmosphere: A case study of α-Cedrene. J Environ Chem Eng. 2024; 12: 112098. https://doi.org/10.1016/j.jece.2024.112098

[35] Li M, Mei Q, Han D, *et al*. The roles of HO·, ClO· and BrO· radicals in caffeine degradation: a theoretical study. Sci Total Environ. 2021; 768: 144733. https://doi.org/10.1016/j.scitotenv.2020.144733

[36] Cristale J, Ramos DD, Dantas RF, *et al*. Can activated sludge treatments and advanced oxidation processes remove organophosphorus flame retardants?. Environ Res. 2016; 144: 11-18. https://doi.org/10.1016/j.envres.2015.10.008

[37] Frisch M, Trucks G, Schlegel H, *et al*. Gaussian 09, Revision A.1. 2009.

[38] Zhao Y, Truhlar DG. The M06 suite of density functionals for main group thermochemistry, thermochemical kinetics, noncovalent interactions, excited states, and transition elements: two new functionals and systematic testing of four M06-class functionals and 12 other functionals. Theor Chem Acc. 2008; 120: 215-241. https://doi.org/10.1007/s00214-007-0310-x

[39] Zhao Y, Truhlar DG. Density functionals with broad applicability in chemistry. Acc Chem Res. 2008; 41: 157-167. https://doi.org/10.1021/ar700111a

[40] Walker M, Harvey AJ, Sen A, *et al*. Performance of M06, M06-2X, and M06-HF density functionals for conformationally flexible anionic clusters: M06 functionals perform better than B3LYP for a model system with dispersion and ionic hydrogen-bonding interactions. J Phys Chem A. 2013; 117: 12590-12600. https://doi.org/10.1021/jp408166m

[41] Fukui K. The path of chemical reactions - the IRC approach. Acc Chem Res. 1981; 14: 363-368. https://doi.org/10.1021/ar00072a001

[42] Canneaux S, Bohr F, Henon E. KiSThelP: A program to predict thermodynamic properties and rate constants from quantum chemistry results. J Comput Chem. 2013; 35: 82-93. https://doi.org/10.1002/jcc.23470

[43] Sanderson H. Probabilistic hazard assessment of environmentally occurring pharmaceuticals toxicity to fish, daphnids and algae by ECOSAR screening. Toxicol Lett. 2003; 144: 383-395. https://doi.org/10.1016/S0378-4274(03)00257-1

[44] Lassalle Y, Jellouli H, Ballerini L, *et al*. Ultraviolet-vis degradation of iprodione and estimation of the acute toxicity of its photodegradation products. J Chromatogr A 2014; 1371: 146-153. https://doi.org/10.1016/j.chroma.2014.10.051

[45] Lu T, Chen F. Multiwfn: A multifunctional wavefunction analyzer. J Comput Chem. 2012; 33: 580-592. https://doi.org/10.1002/jcc.22885

[46] Lu T. A comprehensive electron wavefunction analysis toolbox for chemists, Multiwfn. J Chem Phys. 2024; 161: 082503. https://doi.org/10.1063/5.0216272

[47] Wu L, Chládková B, Lechtenfeld OJ, *et al*. Characterizing chemical transformation of organophosphorus compounds by 13C and 2H stable isotope analysis. Sci Total Environ. 2018; 615: 20-28. https://doi.org/10.1016/j.scitotenv.2017.09.233

[48] Mohammed AR, Adamu U, Gideon S, *et al*. Computational kinetic study on atmospheric oxidation reaction mechanism of 1-fluoro-2-methoxypropane with OH and ClO radicals. J King Saud Univ Sci. 2020; 32: 587-594. https://doi.org/10.1016/j.jksus.2018.08.011

[49] Li C, Chen JW, Xie HB, *et al*. Effects of Atmospheric Water on ·OH-initiated Oxidation of Organophosphate Flame Retardants: A DFT Investigation on TCPP. Environ Sci Technol. 2017; 51: 5043-5051. https://doi.org/10.1021/acs.est.7b00347